

Gnetin C Suppresses MTA1/AKT/mTOR Signaling and Tumor Progression in a Transgenic Mouse Model of Advanced Prostate Cancer

J. Okello^{1*}, M. Ochieng¹, S. Abdi¹

¹Department of Clinical Oncology, Faculty of Medicine, University of Kampala, Kampala, Uganda.

*E-mail ✉ kampala.clinonc.86@emailprovider.net

Received: 05 February 2025; Revised: 21 May 2025; Accepted: 25 May 2025

ABSTRACT

The interplay between metastasis-associated protein 1 and protein kinase B (MTA1/AKT) signaling has been implicated in driving prostate tumor expansion. Plant-derived polyphenols—especially stilbene compounds—have emerged as promising agents for interrupting MTA1-driven prostate malignancy. In this work, we utilized a prostate-specific transgenic mouse line featuring MTA1 overexpression combined with phosphatase and tensin homolog (Pten) deletion (R26MTA1; Pten^{f/f}), as well as PC3M prostate cancer cells, both of which model key alterations found in advanced disease. Mechanistic studies revealed that either silencing MTA1 or chemically suppressing it with gnetin C (a resveratrol dimer) in PC3M cells led to substantial suppression of mammalian target of rapamycin (mTOR) activity. In vivo, mice received daily intraperitoneal injections of gnetin C (7 mg/kg bw) for 12 weeks without exhibiting toxicity. Gnetin C treatment significantly curtailed proliferation and angiogenesis while enhancing apoptosis in mice with late-stage prostate tumors. Moreover, beyond lowering MTA1 expression in prostate epithelial cells, gnetin C strongly diminished mTOR signaling in prostate tissues, including the phosphorylation of mTOR-regulated proteins p70 ribosomal S6 kinase (S6K) and eukaryotic initiation factor 4E (eIF4E)-binding protein 1 (4EBP1). Altogether, these results identify gnetin C as a natural anticancer agent capable of counteracting MTA1/AKT/mTOR-driven prostate cancer, supporting its potential as a standalone therapy or as a complement to approved mTOR inhibitors.

Keywords: Natural compounds, Polyphenols from plants, Gnetin C, Molecular targeting, Antitumor actions, MTA1/mTOR, Advanced prostate malignancy

How to Cite This Article: Okello J, Ochieng M, Abdi S. Gnetin C Suppresses MTA1/AKT/mTOR Signaling and Tumor Progression in a Transgenic Mouse Model of Advanced Prostate Cancer. Asian J Curr Res Clin Cancer. 2025;5(1):124-35. <https://doi.org/10.51847/cXnB3dG3wH>

Introduction

Individuals diagnosed with prostate cancer represent a diverse population whose outcomes range from curable disease to highly aggressive and deadly forms. Between 2007 and 2014, diagnoses declined following adjustments in guidelines for prostate-specific antigen screening, leading to an approximately 5% annual rise in advanced-stage cases [1]. This trend underscores the need to clarify the mechanisms that drive aggressive progression and metastasis. Prostate neoplasms typically originate from precursor lesions such as prostatic intraepithelial neoplasia (PIN), which may evolve into adenocarcinoma and, occasionally, metastatic cancer. Each step of development is marked by distinct molecular features and pathway activation patterns. While androgen receptor (AR) signaling dominates hormone-sensitive disease, tumors that progress after androgen deprivation rely on alternative survival routes, notably the loss of PTEN function and ensuing activation of the AKT/mTOR pathway [2-7]. Another major contributor to advanced disease is MTA1 signaling, which strongly correlates with clinically severe prostate cancer [8, 9]. Our earlier work demonstrated elevated MTA1 levels in Pten-deficient mouse models, influencing inflammation and survival pathways [10]. We previously showed that reduced MTA1 expression was associated with increased PTEN acetylation and activation, thereby limiting disease progression partly by inhibiting p-AKT—revealing a deregulated MTA1/PTEN/AKT axis in prostate cancer [10, 11]. More recently, studies in a

pre-malignant high-risk model (R26MTA1; Pten^{+/f}; Pb-Cre⁺) showed that dietary stilbenes such as pterostilbene and gnetin C (resveratrol dimer) prevented progression from high-grade PIN to adenocarcinoma [12, 13].

Despite extensive efforts to develop inhibitors targeting PI3K/AKT/mTOR, clinical trials in prostate cancer have been hindered by toxicity [14] and limited therapeutic benefit [15]. Interest in natural polyphenols has grown over the last two decades due to their anti-inflammatory and anticancer effects [16-18]. Multiple classes of these compounds can modulate pathways, including PI3K/AKT/mTOR [19-21]. Our team has consistently documented the MTA1-dependent anticancer actions of stilbenes—resveratrol, pterostilbene, and gnetin C [10, 22]—and has recently shown gnetin C to suppress tumor growth in xenografts and act as a preventive agent in a transgenic model [13, 23]. Based on this foundation, we proposed that gnetin C could function as a targeted MTA1 inhibitor for advanced prostate cancer. Such an approach would offer two advantages: (1) biomarkers like MTA1 within the AKT/mTOR axis may identify patients likely to respond to non-kinase-based pathway inhibitors; and (2) a well-tolerated natural compound that blocks MTA1-linked signaling could support innovative, low-toxicity combination strategies.

In this study, our goals were to: (1) generate a genetically engineered mouse model that mirrors advanced prostate cancer arising from prostate-specific MTA1 overexpression together with PTEN loss (R26MTA1; Pten^{f/f}; Pb-Cre⁺; hereafter R26MTA1; Pten^{f/f}); (2) determine the downstream signaling alterations resulting from MTA1 overexpression in PTEN-deficient tumors and define how they foster tumor progression; and (3) evaluate how effectively gnetin C modulates MTA1-controlled pathways *in vivo*.

Materials and Methods

Reagents and cell culture

Gnetin C was supplied by Hosoda SHC Co., Ltd. (Fukui, Japan). For all experiments, the compound was prepared in dimethyl sulfoxide (DMSO) at a final concentration of 0.1% for *in vitro* tests and 10% for *in vivo* treatments, then stored in light-protected conditions at -20 °C.

PC3M prostate cancer cells were obtained from Dr. R. Bergman (University of Nebraska Medical Center, Omaha, NE, USA). Cultures were maintained in RPMI-1640 supplemented with 10% fetal bovine serum under standard incubation conditions (37 °C, 5% CO₂). MTA1-silenced PC3M derivatives were produced according to a previously published protocol [24] using three shRNA constructs, with clone #3 selected for this study due to the strongest knockdown. All lines were confirmed to be free of mycoplasma contamination with the Universal Mycoplasma Detection Kit (ATCC, Manassas, VA, USA).

RNA sequencing

RNA-Seq was carried out on prostates from 18-week-old animals representing four genotypes:

1. R26MTA1; Pb-Cre⁻ (WT)
2. R26MTA1; Pb-Cre⁺ (MTA1 OE)
3. Pten^{f/f}; Pb-Cre⁺ (Pten-null)
4. R26MTA1; Pten^{f/f}; Pb-Cre⁺ (Pten-null MTA1 OE)

Genotypes were validated by PCR using previously established primer sets [12]. Total RNA was extracted with the miRNeasy Kit (Qiagen, Hilden, Germany) and sent to LC Sciences (Houston, TX, USA) for library preparation and sequencing.

Two independent biological replicates were processed per genotype. Sequencing reads were aligned to the GRCm39 reference transcriptome (Ensembl; accessed 22 March 2023) and summarized to gene-level counts using biomaRt (Bioconductor; accessed 22 March 2023).

Differentially expressed genes (DEGs) were identified with DESeq2 [25] using FDR < 0.05 and |log₂FC| ≥ 1. Pathway enrichment was evaluated with the MSigDB Hallmark sets [26], also applying FDR < 0.05.

Western blot analysis

Protein lysates from both cultured cells and prostate tissues were separated on 6%, 10%, or 15% polyacrylamide gels and transferred to PVDF membranes following previously published methods [13]. Primary antibodies targeting MTA1, AKT, p-AKT^{Ser473}, mTOR, p-mTOR^{S2448}, p-S6K^{T389}, p-4EBP1, and Cyclin D1 (Cell

Signaling Technology, Beverly, MA, USA) were used. β -actin and HSP70 (Santa Cruz Biotechnology, Dallas, TX, USA) served as loading controls.

Signals were visualized using enhanced chemiluminescence on a Bio-Rad ChemiDoc system and quantified with ImageJ v1.54h (NIH, Bethesda, MD, USA) as phospho/total protein ratios normalized to loading controls.

Animals and study design

All procedures were approved by the Long Island University IACUC (protocol #2022-011, approved 10 March 2022). Mice were housed under pathogen-free conditions with unlimited access to food and water and were observed daily for overall health.

Mouse models

The R26MTA1; Pb-Cre⁺ model with biallelic MTA1 overexpression in the prostate was described previously [12]. These animals were crossed with C57BL/6J Pten^{f/f} mice (Jackson Laboratories, Nashville, TN, USA) to produce R26MTA1; Pten^{+/f}; Pb-Cre⁺ [12, 13] and R26MTA1; Pten^{f/f}; Pb-Cre⁺ males for the present work. Tail-DNA genotyping used the following primers:

- MTA1 F: 5'-GCT GCT CTC ATC CTC AGA AAC C-3'
- MTA1 R: 5'-CTC GAT GTT GTG GCG GAT CTT GAA GTT-3' (715 bp)
- PTEN F: 5'-CAA GCA CTC TGC GAA CTG AG-3'
- PTEN R: 5'-AAG TTT TTG AAG GCA AGA TGC-3' (156 bp WT, 328 bp mutant)
- Cre F: 5'-TCG CGA TTA TCT TCT ATA TCT TCA G-3'
- Cre R: 5'-GCT CGA CCA GTT TAG TTA CCC-3' (392 bp) [12]

PCRs were run on an Eppendorf thermocycler. A reference group of R26MTA1; Pb-Cre⁻ males (n = 3) with normal prostates served as baseline controls.

experimental design

Dose rationale: Previous studies showed that pterostilbene delivered intraperitoneally at 10 mg/kg bw produced anticancer effects without toxicity [10]. Considering gnetin C's improved pharmacokinetics [27] and demonstrated safety in rodents [28], a daily dose of 7 mg/kg bw was chosen.

Using the standard animal-to-human conversion equation

$$\text{HED (mg/kg)} = \text{animal dose} \times \text{Km}, \quad (1)$$

with Km = 0.081 for mice [29], the selected dose corresponds to 39.69 mg/day for a 70-kg adult male—consistent with levels tolerated in human studies [27, 30-32].

Two cohorts of R26MTA1; Pten^{f/f} mice were assigned at 3–4 weeks of age:

- Vehicle group: 10% DMSO, n = 7
- Gnetin C group: 7 mg/kg bw/day, n = 11

Mice received intraperitoneal injections 5 days per week, followed by 2 days off, for a total of 12 weeks. Body weights and general condition were monitored daily.

At the study endpoint, euthanasia was performed according to IACUC requirements. Owing to the small prostate size, animals within each group were divided such that some contributed UGS tissues (prostate, seminal vesicles, bladder) for histology/IHC, while others provided prostate samples for protein extraction and storage at -80 °C. Blood was collected by cardiac puncture, and serum was stored at -80 °C.

Histology and immunohistochemistry analyses of prostate tissues

Formalin-fixed, paraffin-embedded prostate samples (Reveal Biosciences, San Diego, CA, USA) were processed and stained with hematoxylin and eosin (H&E) for independent microscopic evaluation (GC and CY). A board-certified veterinary pathologist (CY) graded the extent of prostatic intraepithelial neoplasia (PIN) and adenocarcinoma using the following scheme: Score 0: absence of detectable PIN or carcinoma; Score 1: presence of PIN only; Score 2: coexistence of PIN and adenocarcinoma with carcinoma comprising <50% of the gland; Score 3: PIN plus adenocarcinoma with carcinoma involving >50% of the prostate. For each mouse, at least five

randomly selected regions from distinct prostate areas were examined, and phenotype assessments were based on multiple tissue sections.

Slides underwent immunohistochemical staining with antibodies targeting Ki67, MTA1, CD31, cleaved caspase-3 (CC3), p-mTOR, p-S6K, and p-4EBP1. In brief, sections were deparaffinized, rehydrated, and subjected to antigen retrieval. Serum was used to block nonspecific binding, and endogenous peroxidase activity was suppressed. Primary antibodies were applied overnight, followed by secondary antibodies and an avidin–biotin complex (Vectastain ABC Elite Kit, Vector Laboratories, Newark, CA, USA). Color development was achieved with the ImmPACT DAB system (Vector Laboratories). Images were acquired with an EVOS XL Core microscope (Thermo Fisher Scientific, Somerset, NJ, USA). Marker staining intensity was assessed and scored by GC. Ki67 quantification was based on the proportion of positively stained nuclei. Cytoplasmic and nuclear staining was rated on a four-level scale: 1 (weak), 2 (fair), 3 (moderate), and 4 (strong). For each group, a minimum of five randomly chosen fields per sample was analyzed using ImageJ v1.54h (NIH, Bethesda, MD, USA) or QuPath v0.5.0. ImageJ supported cell counting and measurement of CD31-labeled vascular area (mm²), whereas QuPath facilitated automated quantification of PIN and carcinoma severity.

ELISA

Serum IL-2 concentrations were measured from 50 µL samples using a commercial ELISA kit (Abcam, Boston, MA, USA) as previously reported [12, 13]. Standards and samples were plated in duplicate, incubated with the antibody mixture, and detected using 3, 3', 5, 5'-tetramethylbenzidine substrate. Absorbance was recorded at 450 nm using a microplate reader (Tecan, Mannedorf, Switzerland). IL-2 levels were calculated through interpolation from a standard curve.

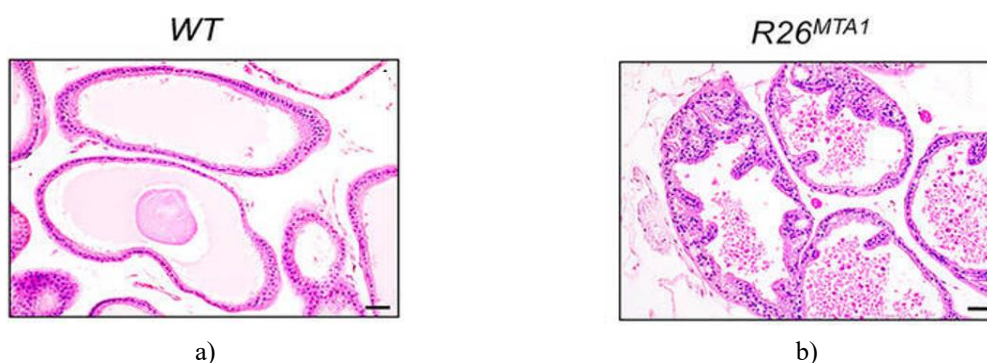
Statistical analysis

All statistical testing was conducted using GraphPad Prism v9 (San Diego, CA, USA). Depending on the comparison, either Student's t-test or one-way ANOVA was applied. Results are expressed as mean ± SEM, and $p < 0.05$ was considered statistically significant.

Results and Discussion

*Prostate-specific MTA1 overexpression drives invasive adenocarcinoma in *pten*^{ff} mice*

Prior work indicates that elevated MTA1 expression in the prostate accelerates the emergence of PIN in *Pten*^{+/f} animals [12, 13]. We therefore posited that enhancing MTA1 expression in a complete PTEN-loss background (*Pten*^{f/f}) would worsen disease progression and potentially support metastasis. To test this, we established a prostate-targeted R26MTA1; *Pten*^{f/f} model, which develops PIN that advances to adenocarcinoma. The incidence of glands exhibiting carcinoma versus PIN was similar between R26MTA1; *Pten*^{f/f} and *Pten*^{f/f} mice. Likewise, increased MTA1 did not markedly alter tumor development kinetics under PTEN-deficiency, and neither renal nor iliac lymph node metastases were detected even at 36 weeks. Morphologically, prostates lacking PTEN and overexpressing MTA1 exhibited well to moderately differentiated invasive adenocarcinoma, with malignant epithelial cells forming gland-like structures accompanied by desmoplastic stromal responses and varied inflammatory infiltrates (lymphocytes, plasma cells, and neutrophils). No evidence of lymphovascular invasion was observed. Tumor cells breaching the basement membrane did not acquire a spindle-cell phenotype (**Figure 1**).



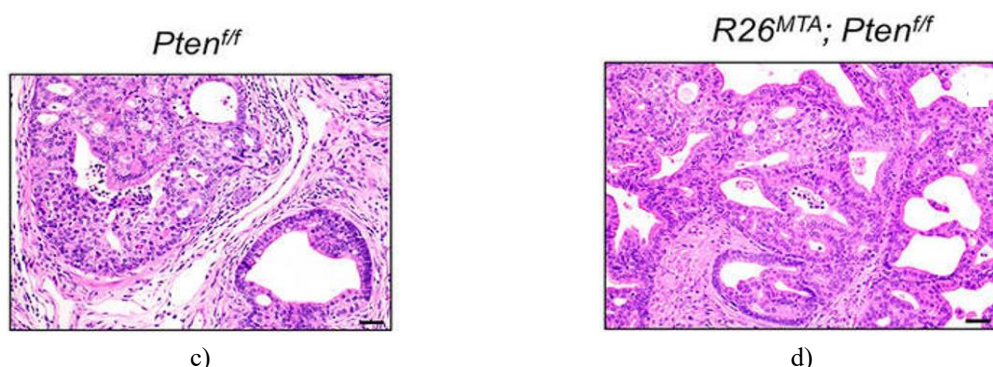


Figure 1. Representative micrographs of prostates from four genotypes—(a) R26MTA1; Pb-Cre-negative (WT), (b) R26MTA1, (c) *Pten*^{f/f}, and (d) R26MTA1; *Pten*^{f/f}—stained with H&E (scale bar: 100 μm). WT prostates appear normal. R26MTA1 mice occasionally show epithelial hyperplasia without cytologic atypia. Both *Pten*^{f/f} and R26MTA1; *Pten*^{f/f} mice display PIN and adenocarcinoma. The lower panels illustrate well to moderately differentiated invasive adenocarcinoma with stromal desmoplasia and inflammatory cells.

To identify transcriptional programs altered by prostate-specific MTA1 elevation, RNA-Seq was performed on mouse prostate tissue. Compared with *Pten*^{f/f} controls, R26MTA1; *Pten*^{f/f} prostates showed substantial changes: 867 genes were significantly upregulated and 1088 downregulated (FDR < 0.05). A heatmap illustrating gene clustering between the groups is presented in **Figure 2a**. Among the pathways most influenced by MTA1 overexpression under PTEN loss was the mTORC1 (mTOR) signaling pathway (**Figure 2b**), which is well recognized for its aberrant activation in castration-resistant and advanced PTEN-deficient prostate cancer [14, 33]. Thus, the R26MTA1; *Pten*^{f/f} model reflects a subset of advanced prostate tumors characterized by heightened mTOR activity, supporting the possibility that targeting the MTA1/mTOR axis with the natural stilbene gnetin C may impede disease advancement.

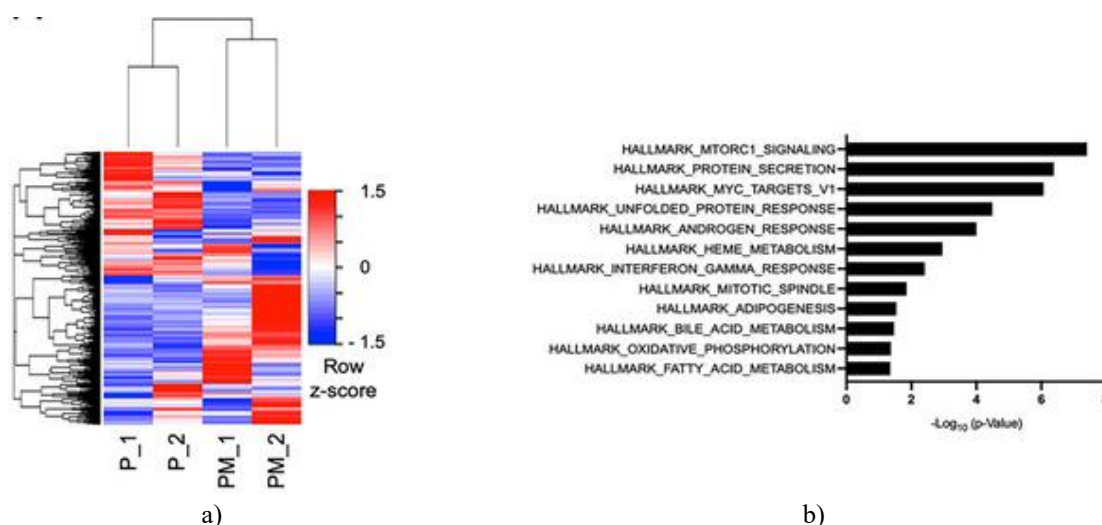


Figure 2. (a) Heatmap of DEGs in R26MTA1; *Pten*^{f/f} (PM_1 and PM_2) relative to *Pten*^{f/f} (P_1 and P_2). (b) Gene-set enrichment analysis (Hallmark sets, MSigDB) for DEGs comparing the two groups.

Suppression of the MTA1/mTOR cascade by gnetin C in cultured cells

To begin clarifying how the MTA1/mTOR axis is regulated, we initially examined the functional association between MTA1 and mTOR signaling in PC3M prostate cancer cells, which exhibit a PTEN-null genotype [34] and display the highest MTA1 abundance among prostate cancer cell models [8]. In tumor biology, the AKT/mTOR pathway operates through both mTORC1 and mTORC2: mTORC1 governs cellular expansion by modulating S6K and 4EBP1, while mTORC2 activates AKT phosphorylation, supporting cell viability [14, 35]. Elevated mTOR activity, marked by phosphorylated S6K and 4EBP1, has been linked with increased CyclinD1 [36-38], whereas blocking PI3K/AKT/mTOR/S6K signaling reduces CyclinD1 within malignant cells [38, 39].

Western blot assessment of mTOR-associated proteins showed that PC3M cells with MTA1 knockdown had a sharp decline in p-AKT, p-mTOR, and their downstream effectors (p-S6K, p-4EBP1, and CyclinD1) relative to non-silenced controls, indicating that MTA1 operates upstream of mTOR (**Figures 3a and 3c**). These data imply that MTA1-driven stimulation of the mTOR/S6K/4EBP1/CyclinD1 circuitry could underlie prostate tumor progression in PTEN-deficient settings, supporting a direct positive interaction between MTA1 and mTOR independent of the MTA1/PTEN relationship [11]. Consistent with earlier findings showing that Gnetin C has an IC₅₀ of 8.7 μ M in PC3M cells [26, 27], treatment with this compound lowered MTA1 and diminished p-mTOR, p-S6K, p-4EBP1, and CyclinD1 levels (**Figures 3b and 3d**), highlighting that gnetin C pharmacologically attenuates the MTA1/mTOR pathway.

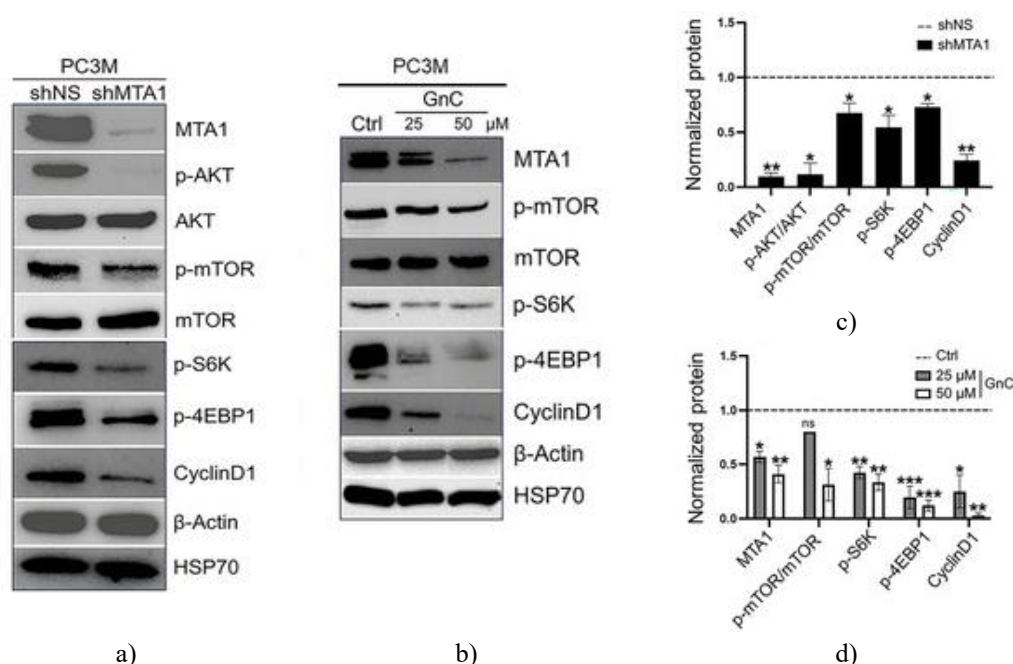
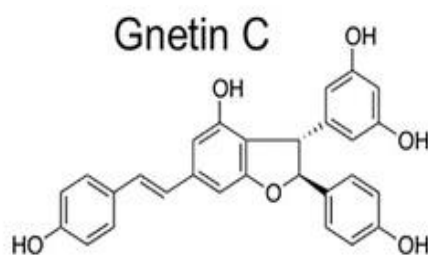


Figure 3. (a) Western blot evaluation and quantification of markers in MTA1-expressing (shNS) vs. MTA1-silenced (shMTA1) PC3M cells. (b) Dose-dependent inhibition of pathway markers by gnetin C. β -actin and HSP70 served as loading controls. (c) Quantification of markers in shNS vs. shMTA1 cells. (d) Quantification of responses to 25 and 50 μ M gnetin C. Data represent mean \pm SEM from three experiments. * $p < 0.05$; ** $p < 0.01$; *** $p < 0.001$; ns = not significant. Uncropped images appear in File S1.

Gnetin C administration reduces adenocarcinoma development in R26MTA1; pten^{fl/f} mice

When 18 R26MTA1; Pten^{fl/f} mice were available, 4-week-old animals were randomly divided into two cohorts: vehicle-treated ($n = 7$) or gnetin C-treated (7 mg/kg body weight; $n = 11$) via intraperitoneal injection for 12 weeks. At week 13, animals were euthanized, and prostate tissue and blood were harvested for downstream analyses (**Figure 4**). Cre-negative littermates functioned as reference controls. Health status and body mass were followed throughout, with no detectable toxicity.



a)

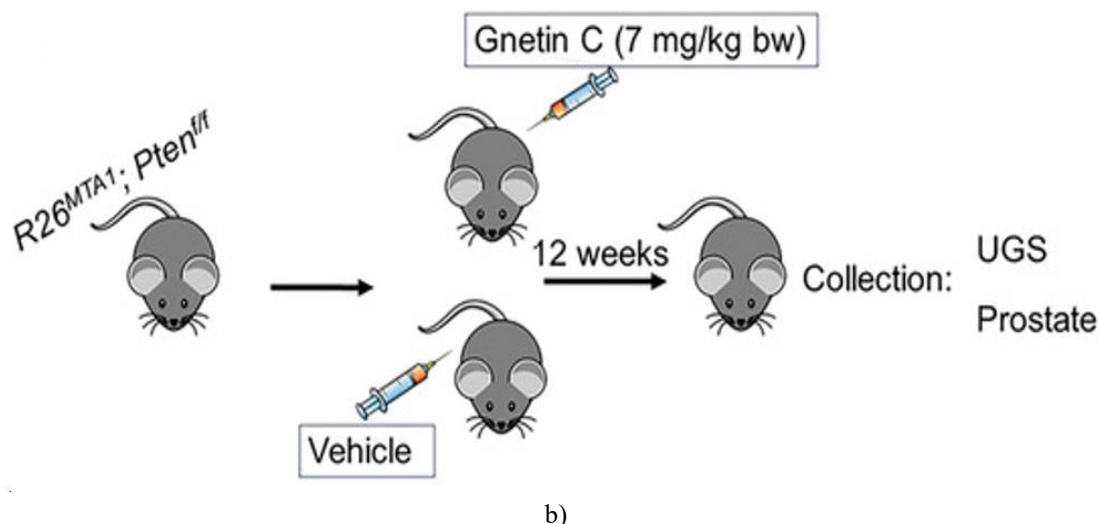


Figure 4. (a) Chemical depiction of gnetin C. (b) Outline of treatment protocol used to evaluate therapeutic effects in the advanced prostate cancer mouse model. *R26MTA1; Pten^{f/f}* mice received vehicle ($n = 7$) or gnetin C (7 mg/kg per day) ($n = 11$) for 12 weeks before UGS or prostate samples were processed for histological and molecular evaluations.

As illustrated in **Figure 5a** (top), the vehicle cohort predominantly displayed adenocarcinoma, identified by invasive neoplastic glandular epithelial proliferation, disruption of the basement membrane, desmoplastic stroma, and moderate-to-large infiltration of neutrophils, lymphocytes, and plasma cells. No lymphovascular invasion was observed, and invading tumor cells did not adopt a spindle-like morphology. Conversely, gnetin C–treated mice showed a higher proportion of PIN lesions, characterized by glandular proliferation without stromal invasion and minimal inflammatory infiltrates. Immunohistochemistry in the gnetin C group revealed clear reductions in Ki67 and CD31, indicating reduced proliferation and angiogenesis, while CC3 staining confirmed enhanced apoptosis relative to controls (**Figure 5a**). Further, gnetin C therapy led to lowered MTA1 and diminished activation of p-mTOR, p-S6K, and p-4EBP1 (**Figure 5b**).

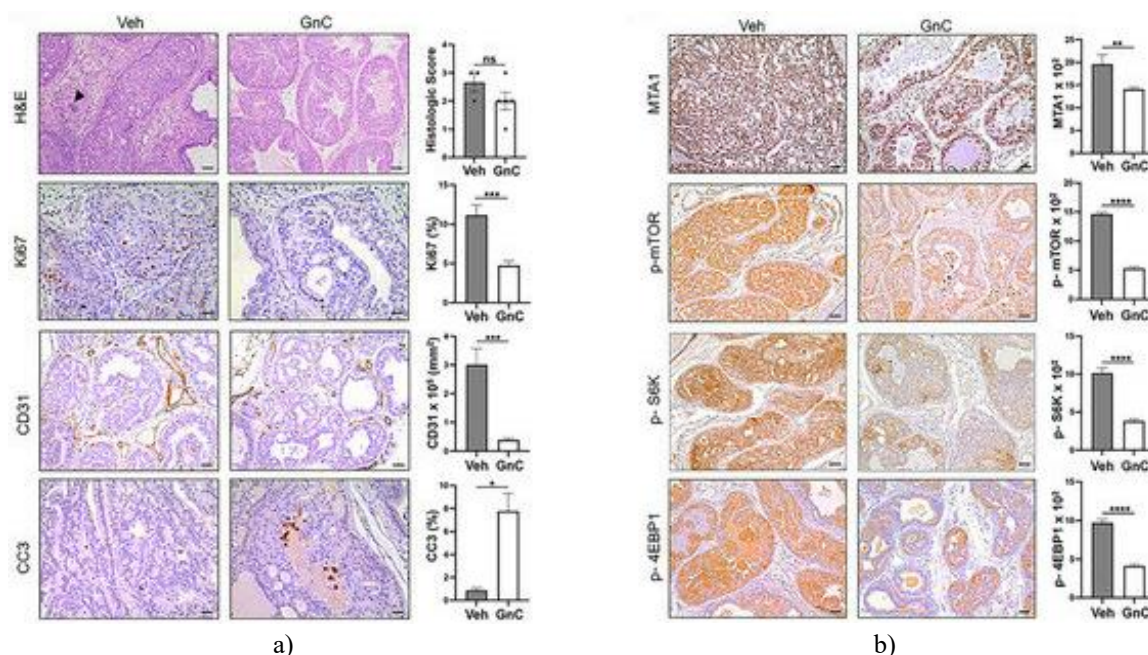


Figure 5. (a) Left: H&E and IHC images (scale bars: H&E = 50 μ m; Ki67/CC3 = 20 μ m; CD31 = 50 μ m). Right: Quantification of PIN vs. adenocarcinoma and IHC markers. (b) Left: Representative staining for MTA1/mTOR pathway components in vehicle vs. gnetin C–treated prostates. Right: Quantification of

MTA1, p-mTOR, p-S6K, and p-4EBP1; mean \pm SEM from 5–7 regions per sample (Veh, $n = 3$; GnC, $n = 5$).
* $p < 0.05$; ** $p < 0.01$; *** $p < 0.001$; **** $p < 0.0001$; ns = not significant.

To expand these observations, pathway-related proteins were also examined in prostate lysates via Western blotting (**Figure 6a**). Despite some sample-to-sample variation, levels of MTA1, p-4EBP1, and CyclinD1 were consistently suppressed in gnetin C-treated prostates when compared with vehicle controls. Interestingly, p-mTOR and total mTOR signals did not show a treatment-associated pattern. This may stem partly from limited sample availability and also from prior clinical data reporting that elevated p-mTOR/mTOR levels in prostate cancer patients correlate with better outcomes [40, 41]. The inconsistent significance of p-mTOR/mTOR in this disease may contribute to the modest therapeutic performance of PI3K/AKT/mTOR inhibitors [14, 40, 41]. Nonetheless, assessing MTA1, p-4EBP1, and CyclinD1 in clinical settings may help identify individuals with high MTA1 expression who are more likely to respond to gnetin C-based interventions.

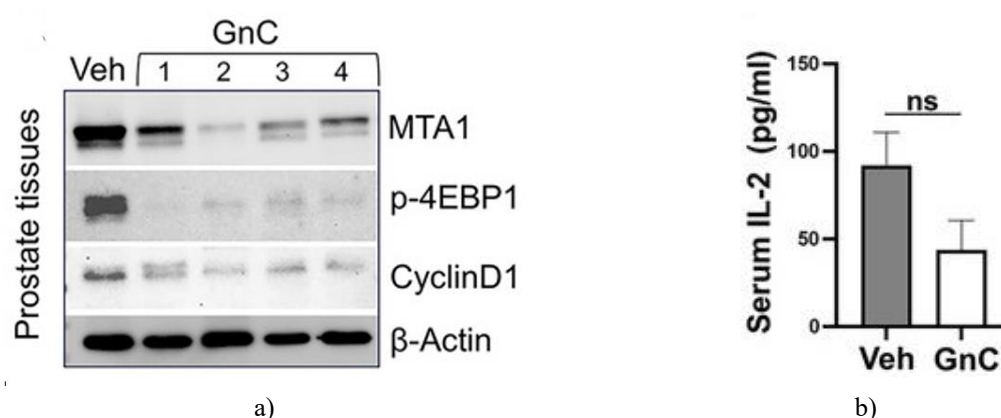


Figure 6. (a) Sample Western blot panels showing how gnetin C (GnC) suppresses MTA1/mTOR-related proteins in prostate tissue from differently treated mice. β -actin served as the loading reference. (b) Serum IL-2 concentrations in mice ($n = 4$ per group) assessed via ELISA. Values are presented as mean \pm SEM from three independent, duplicate-performed experiments. ns = not significant; Veh = vehicle.

Uncropped images appear in File S1.

We next assessed whether gnetin C alters inflammatory signaling in R26MTA1; *Pten*^{f/f} animals by measuring circulating IL-2 (**Figure 6b**). Similar to earlier findings from a high-risk PIN model receiving low-dose dietary gnetin C [13], the present study also revealed a reduction in IL-2 in GnC-treated mice relative to vehicle controls. Overall, our findings indicate that gnetin C administration improves pathological features in R26MTA1; *Pten*^{f/f} mice, producing a significant decline in MTA1 expression together with reduced proliferation and angiogenesis, enhanced apoptosis, and clear inhibition of MTA1-linked markers of activated mTOR signaling, supported by both IHC and Western blot evidence. These results highlight that gnetin C exhibits multiple advantageous activities—including anti-inflammatory and anticancer effects—establishing its therapeutic potential in a preclinical model of advanced prostate cancer.

Although mTOR-targeting drugs have shown success in several malignancies [42–44], they have been considerably less effective in prostate cancer [14, 45, 46], and toxicity associated with these agents underscores the urgency for safer and more precise therapeutic options [14, 44].

In this work, we sought a natural inhibitor of the mTOR cascade suitable for prostate cancer treatment by employing a clinically meaningful murine system. The prostate-restricted R26MTA1; *Pten*^{f/f} genetically engineered line models PTEN-loss-driven advanced cancer, driven further by heightened MTA1 expression. Earlier studies from our group demonstrated a negative relationship between PTEN activity and MTA1 levels, producing abnormal AKT signaling [10, 11]. Here, we examined the direct connection between MTA1 and AKT's downstream effector—the mTOR pathway—and found that MTA1 serves as an upstream regulator of mTOR independent of PTEN status. Supporting this, a recent report on endometrial cancer identified the miR-30c/MTA1 axis as a controller of cell proliferation, motility, and invasion through AKT/mTOR/4EBP1 signaling, positioning MTA1 as a therapeutic target [47].

Importantly, this is the first demonstration of pharmacologic modulation of the MTA1/mTOR network using gnetin C both in vitro and in vivo. Our data show that gnetin C markedly reduces MTA1 and diminishes phosphorylation of AKT, mTOR, S6K, 4EBP1, and CyclinD1 in PC3M cells. Within prostate tissue—despite limited sample availability—GnC significantly decreased MTA1, p-4EBP1, and CyclinD1. Given the elaborate nature of mTOR network regulation in prostate malignancies, it is expected that in vivo responses may reflect this complexity. This highlights the need for additional mTOR-related biomarkers that can predict therapeutic response. Notably, suppression of MTA1 by gnetin C produced consistent downregulation of p-S6K, p-4EBP1, and CyclinD1 across IHC and Western blot analyses.

Our observations align with earlier leukemia studies demonstrating gnetin C's capacity to inhibit AKT/mTOR and ERK1/2 pathways in cell lines, patient-derived samples, and animal models. That work also showed that combining gnetin C with low doses of chemotherapeutics yields synergistic antitumor effects [28].

Going forward, chemically modifying gnetin C to enhance its pharmacokinetic behavior may strengthen its efficacy as a single agent. Additionally, gnetin C or its derivatives—owing to their chemosensitizing properties—may synergize with approved therapies. We recently showed that gnetin C acts together with enzalutamide to restrict proliferation and angiogenesis while increasing apoptosis in a castration-resistant xenograft model through dual targeting of AR-V7 and MTA1 [48]. While selective MTA1 inhibitors are not currently available, existing mTOR inhibitors such as rapamycin derivatives could be used in combination at lower doses. Thus, future combined therapeutic strategies could benefit subsets of patients displaying MTA1/mTOR pathway activation. More research is needed to determine how tumor heterogeneity in MTA1 expression affects treatment outcomes and whether phosphorylated signaling proteins can reliably predict combination therapy responsiveness.

Conclusion

The R26MTA1; Ptenf/f model reproduces the principal features of advanced prostate cancer driven by aberrant MTA1/mTOR signaling and offers a valuable platform for evaluating emerging therapies. Identifying a natural mTOR inhibitor with strong activity and low toxicity broadens the translational promise of targeting this pathway. Collectively, our results demonstrate that the natural stilbene gnetin C is a highly effective inhibitor of the MTA1/mTOR axis in a preclinical setting and may help impede disease progression in patients whose tumors exhibit dysregulated MTA1/PTEN/AKT/mTOR signaling (**Figure 7**). Natural bioactive compounds such as gnetin C that modulate specific oncogenic pathways may represent important future directions for treating advanced prostate cancer.

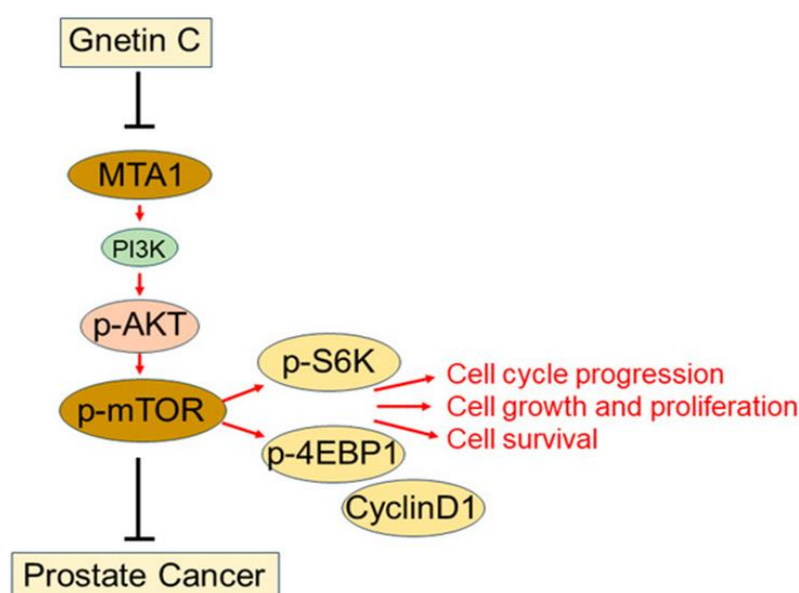


Figure 7. Overview of the MTA1/mTOR signaling circuit in prostate cancer. In the R26MTA1; Ptenf/f model, elevated MTA1 enhances mTOR activation, driving phosphorylation of S6K, 4EBP1, and CyclinD1, which together support tumor cell growth, division, and survival. Gnetin C, a plant-derived stilbene, disrupts this MTA1-dependent mTOR activation and exhibits strong antitumor effects.

Acknowledgments: None

Conflict of Interest: None

Financial Support: None

Ethics Statement: None

References

1. Siegel RL, Miller KD, Wagle NS, Jemal A. Cancer statistics, 2023. *CA Cancer J Clin.* 2023;73(1):17-48.
2. Malik SN, Brattain M, Ghosh PM, Troyer DA, Prihoda T, Bedolta R, et al. Immunohistochemical demonstration of phospho-Akt in high Gleason grade prostate cancer. *Clin Cancer Res.* 2002;8(4):1168-71.
3. Pawletz CP, Charboneau L, Bichsel VE, Simone NL, Chen T, Gillespie JW, et al. Reverse phase protein microarrays which capture disease progression show activation of pro-survival pathways at the cancer invasion front. *Oncogene.* 2001;20(16):1981-9.
4. Kim MJ, Cardiff RD, Desai N, Banach-Petrosky WA, Parsons R, Shen MM, et al. Cooperativity of Nkx3.1 and Pten loss of function in a mouse model of prostate carcinogenesis. *Proc Natl Acad Sci U S A.* 2002;99(4):2884-9.
5. Grant S. Cotargeting survival signaling pathways in cancer. *J Clin Invest.* 2008;118(9):3003-6.
6. Shorning BY, Dass MS, Smalley MJ, Pearson HB. The PI3K-AKT-mTOR pathway and prostate cancer: At the crossroads of AR, MAPK, and WNT signaling. *Int J Mol Sci.* 2020;21(12):4507.
7. Kinkade CW, Castillo-Martin M, Puzio-Kuter A, Yan J, Foster TH, Gao H, et al. Targeting AKT/mTOR and ERK MAPK signaling inhibits hormone-refractory prostate cancer in a preclinical mouse model. *J Clin Invest.* 2008;118(9):3051-64.
8. Dias SJ, Zhou X, Ivanovic M, Gailey MP, Dhar S, Zhang L, et al. Nuclear MTA1 overexpression is associated with aggressive prostate cancer, recurrence and metastasis in African Americans. *Sci Rep.* 2013;3:2331.
9. Hofer MD, Kuefer R, Varambally S, Li H, Ma J, Shapiro GI, et al. The role of metastasis-associated protein 1 in prostate cancer progression. *Cancer Res.* 2004;64:825-9.
10. Dhar S, Kumar A, Zhang L, Rimando AM, Lage JM, Lewin JR, et al. Dietary pterostilbene is a novel MTA1-targeted chemopreventive and therapeutic agent in prostate cancer. *Oncotarget.* 2016;7:18469-84.
11. Dhar S, Kumar A, Li K, Tzivion G, Levenson AS. Resveratrol regulates PTEN/Akt pathway through inhibition of MTA1/HDAC unit of the NuRD complex in prostate cancer. *Biochim Biophys Acta.* 2015;1853:265-75.
12. Hemani R, Patel I, Inamdar N, Campanelli G, Donovan V, Kumar A, et al. Dietary pterostilbene for MTA1-targeted interception in high-risk premalignant prostate cancer. *Cancer Prev Res.* 2022;15(1):87-100.
13. Parupathi P, Campanelli G, Deabel RA, Puaar A, Devarakonda LS, Kumar A, et al. Gnetin C intercepts MTA1-associated neoplastic progression in prostate cancer. *Cancers.* 2022;14(23):6038.
14. Choudhury AD. PTEN-PI3K pathway alterations in advanced prostate cancer and clinical implications. *Prostate.* 2022;82(Suppl S1):S60-72.
15. Braglia L, Zavatti M, Vinceti M, Martelli AM, Marmiroli S. Deregulated PTEN/PI3K/AKT/mTOR signaling in prostate cancer: Still a potential druggable target? *Biochim Biophys Acta Mol Cell Res.* 2020;1867(1):118731.
16. Asensi M, Ortega A, Mena S, Feddi F, Estrela JM. Natural polyphenols in cancer therapy. *Crit Rev Clin Lab Sci.* 2011;48(1):197-216.
17. Rudzinska A, Juchaniuk P, Oberda J, Wisniewska J, Wojdan W, Szklener K, et al. Phytochemicals in cancer treatment and cancer prevention—Review on epidemiological data and clinical trials. *Nutrients.* 2023;15(8):1896.
18. Swetha M, Keerthana CK, Rayginia TP, Anto RJ. Cancer chemoprevention: A strategic approach using phytochemicals. *Front Pharmacol.* 2021;12:809308.
19. Tewari D, Patni P, Bishayee A, Sah AN, Bishayee A. Natural products targeting the PI3K-Akt-mTOR signaling pathway in cancer: A novel therapeutic strategy. *Semin Cancer Biol.* 2022;30:1-17.

20. Narayanankutty A. Inhibitory potential of dietary nutraceuticals on cellular PI3K/Akt signaling: Implications in cancer prevention and therapy. *Curr Top Med Chem.* 2021;21(17):1816–31.
21. Narayanankutty A. Phytochemicals as PI3K/Akt/mTOR inhibitors and their role in breast cancer treatment. *Recent Pat Anticancer Drug Discov.* 2020;15(3):188–99.
22. Levenson AS. Metastasis-associated protein 1-mediated antitumor and anticancer activity of dietary stilbenes for prostate cancer chemoprevention and therapy. *Semin Cancer Biol.* 2020;80:107–17.
23. Gadkari K, Kolhatkar U, Hemani R, Campanelli G, Cai Q, Kumar A, et al. Therapeutic potential of Gnetin C in prostate cancer: A pre-clinical study. *Nutrients.* 2020;12(12):3631.
24. Kumar A, Dholakia K, Sikorska G, Martinez LA, Levenson AS. MTA1-dependent anticancer activity of Gnetin C in prostate cancer. *Nutrients.* 2019;11(9):2096.
25. Love MI, Huber W, Anders S. Moderated estimation of fold change and dispersion for RNA-seq data with DESeq2. *Genome Biol.* 2014;15(12):550.
26. Liberzon A, Birger C, Thorvaldsdottir H, Ghandi M, Mesirov JP, Tamayo P. The Molecular Signatures Database (MSigDB) hallmark gene set collection. *Cell Syst.* 2015;1(6):417–25.
27. Tani H, Hikami S, Iizuna S, Yoshimatsu M, Asama T, Ota H, et al. Pharmacokinetics and safety of resveratrol derivatives in humans after oral administration of melinjo (*Gnetum gnemon* L.) seed extract powder. *J Agric Food Chem.* 2014;62(9):1999–2007.
28. Espinoza JL, Elbadry MI, Taniwaki M, Harada K, Trung LQ, Nakagawa N, et al. The simultaneous inhibition of the mTOR and MAPK pathways with Gnetin-C induces apoptosis in acute myeloid leukemia. *Cancer Lett.* 2017;400:127–36.
29. Nair AB, Jacob S. A simple practice guide for dose conversion between animals and human. *J Basic Clin Pharm.* 2016;7(2):27–31.
30. Nakagami Y, Suzuki S, Espinoza JL, Vu Quang L, Enomoto M, Takasugi S, et al. Immunomodulatory and metabolic changes after Gnetin-C supplementation in humans. *Nutrients.* 2019;11(6):1403.
31. Konno H, Kanai Y, Katagiri M, Watanabe T, Mori A, Ikuta T, et al. Melinjo (*Gnetum gnemon* L.) seed extract decreases serum uric acid levels in nonobese Japanese males: A randomized controlled study. *Evid Based Complement Alternat Med.* 2013;2013:589169.
32. Espinoza JL, An DT, Trung LQ, Yamada K, Nakao S, Takami A, et al. Stilbene derivatives from melinjo extract have antioxidant and immune modulatory effects in healthy individuals. *Integr Mol Med.* 2015;2(6):405–13.
33. Bitting RL, Armstrong AJ. Targeting the PI3K/Akt/mTOR pathway in castration-resistant prostate cancer. *Endocr Relat Cancer.* 2013;20(2):R83–99.
34. Sharrard RM, Maitland NJ. Regulation of protein kinase B activity by PTEN and SHIP2 in human prostate-derived cell lines. *Cell Signal.* 2007;19(1):129–38.
35. Hay N, Sonenberg N. Upstream and downstream of mTOR. *Genes Dev.* 2004;18(16):1926–45.
36. Cai Z, Wang J, Li Y, Shi Q, Jin L, Li S, et al. Overexpressed Cyclin D1 and CDK4 proteins are responsible for the resistance to CDK4/6 inhibitor in breast cancer that can be reversed by PI3K/mTOR inhibitors. *Sci China Life Sci.* 2023;66(1):94–109.
37. Xu Y, Chen SY, Ross KN, Balk SP. Androgens induce prostate cancer cell proliferation through mammalian target of rapamycin activation and post-transcriptional increases in cyclin D proteins. *Cancer Res.* 2006;66(15):7783–92.
38. Recchia AG, Musti AM, Lanzino M, Panno ML, Turano E, Zumpano R, et al. A cross-talk between the androgen receptor and the epidermal growth factor receptor leads to p38MAPK-dependent activation of mTOR and cyclinD1 expression in prostate and lung cancer cells. *Int J Biochem Cell Biol.* 2009;41(3):603–14.
39. Gao N, Flynn DC, Zhang Z, Zhong XS, Walker V, Liu KJ, et al. G1 cell cycle progression and the expression of G1 cyclins are regulated by PI3K/AKT/mTOR/p70S6K1 signaling in human ovarian cancer cells. *Am J Physiol Cell Physiol.* 2004;287(2):C281–91.
40. Stelloo S, Sanders J, Nevedomskaya E, de Jong J, Peters D, van Leenders GJ, et al. mTOR pathway activation is a favorable prognostic factor in human prostate adenocarcinoma. *Oncotarget.* 2016;7(21):32916–24.
41. Barata PC, Magi-Galluzzi C, Gupta R, Dreicer R, Klein EA, Garcia JA, et al. Association of mTOR pathway markers and clinical outcomes in patients with intermediate-/high-risk prostate cancer: Long-term analysis. *Clin Genitourin Cancer.* 2019;17(5):366–72.

42. Jerusalem G, Rorive A, Collignon J. Use of mTOR inhibitors in the treatment of breast cancer: An evaluation of factors that influence patient outcomes. *Breast Cancer*. 2014;6(1):43–57.
43. Battelli C, Cho DC. mTOR inhibitors in renal cell carcinoma. *Therapy*. 2011;8(4):359–67.
44. Hua H, Kong Q, Zhang H, Wang J, Luo T, Jiang Y. Targeting mTOR for cancer therapy. *J Hematol Oncol*. 2019;12(1):71.
45. Edlind MP, Hsieh AC. PI3K-AKT-mTOR signaling in prostate cancer progression and androgen deprivation therapy resistance. *Asian J Androl*. 2014;16(3):378–86.
46. Armstrong AJ, Netto GJ, Rudek MA, Halabi S, Wood DP, Creel PA, et al. A pharmacodynamic study of rapamycin in men with intermediate- to high-risk localized prostate cancer. *Clin Cancer Res*. 2010;16(10):3057–66.
47. Xu X, Kong X, Liu T, Zhou L, Wu J, Fu J, et al. Metastasis-associated protein 1, modulated by miR-30c, promotes endometrial cancer progression through AKT/mTOR/4E-BP1 pathway. *Gynecol Oncol*. 2019;154(1):207–17.
48. Campanelli G, Deabel RA, Puaar A, Devarakonda LS, Parupathi P, Zhang J, et al. Molecular efficacy of Gnetin C as dual-targeted therapy for castrate-resistant prostate cancer. *Mol Nutr Food Res*. 2023;67(1):e2300479.